HENRY

Hydraulic Engineering Repository

Ein Service der Bundesanstalt für Wasserbau

Conference Paper, Published Version

Sokoray-Varga, Béla; Weichert, Roman; Lehmann, Boris; Nestmann, Franz

Detecting turbulent eddies by means of time-resolved piv measurements in a vertical-slot fish pass

Verfügbar unter/Available at: https://hdl.handle.net/20.500.11970/100850

Vorgeschlagene Zitierweise/Suggested citation:
Sokoray-Varga, Béla; Weichert, Roman; Lehmann, Boris; Nestmann, Franz (2012): Detecting turbulent eddies by means of time-resolved piv measurements in a vertical-slot fish pass. In: 2nd IAHR Europe Kongress 'Water infinitely deformable but still limited', 27. - 29. June 2012, TUM Munich. München: Technische Universität München.

DETECTING TURBULENT EDDIES BY MEANS OF PIV IN A VERTICAL-SLOT FISH PASS

Sokoray-Varga Béla[1], Weichert Roman[2], Lehmann Boris[1] & Nestmann Franz[1]

[1]Institute for Water and River Basin Management, Karlsruhe Institute of Technology, Germany, Kaiserstr. 12, 76131 Karlsruhe

[2]Department of Hydraulic Engineering in Inland Areas, Federal Waterways Engineering and Research Institute, Germany, Kussmaulstr. 17, 76187 Karlsruhe

E-mail: sokoray@kit.edu

Abstract

While turbulence in fish passes is commonly indicated as a flow feature influencing fish swimming performance, it is not clearly shown which feature of turbulence is determinative. Since scale effects are suspected to play a major role, our research has the objective to measure features and scales of turbulent eddies in a vertical-slot fish pass. The present paper deals with the applicability of a PIV-system to detect pool-geometry specific turbulent eddies. It shows the preliminary results of a first measurement carried out with a 200 Hz time-resolved PIV-system in a scale model. This system enables both the detection and the tracking of large eddies thought to have the greatest impact on fish swimming.

Introduction

The flow in vertical-slot fish passes has already been investigated with several laboratory experiments with scale models and with in-situ measurements. Most of them have shown that the flow in the fish pass pools becomes highly turbulent due to high velocities and high velocity gradients (e.g. Wu et al., 1999; Puertas et al., 2004; Liu et al., 2006; Tarrade et al., 2008). As turbulence is recognized as a key feature decreasing the swimming performance of fish, the effectiveness of such facilities is certainly determined by the flow conditions in the pools.

The influence of turbulence on fish behavior has been addressed in numerous experiments (e.g. Webb, 1998; Liao et al., 2003; Enders et al., 2003; Nikora et al., 2003; Bleckmann et al., 2004; Silva et al., 2011). However the features of turbulence mainly affecting the swimming behavior have not been clearly identified, scale effects are increasingly suspected behind the disturbance. As a result, recent research has investigated the role of orientation and size of large turbulent eddies on fish (e.g. Smith et al. 2005, Liao 2007, Tritico et al. 2010, Pryzbilla et al. 2010).

However, there is hardly any measurement available for the size and orientation of turbulent eddies in a vertical-slot fish pass. Thus, as long as the eddy characteristics in fish passes are unknown, the findings on fish behavior can not be applied to real fish passes confidently. Moreover, even if certain eddy scales turn out to be disadvantageous for fish, there are hardly any recommendations on how the geometrical modifications of different pool components affect the characteristics of turbulence in the pools.

The ongoing joint research of the Karlsruhe Institute of Technology (KIT) and of the Federal Waterways Engineering and Research Institute (BAW) aims firstly to measure features and scales of the turbulent eddies in a vertical-slot fish pass, and, then, to identify ways of improving turbulence characteristics by modifying the pool geometry.

Capturing turbulent eddies and determining their characteristics is certainly a challenging task, as different measurement techniques capture turbulence differently.

Turbulence should be considered as the superposition of eddies of different time- and length- scales.

On the one hand, point-measurement techniques, like Acoustic Doppler Velocimetry (ADV), detect turbulence as local velocity fluctuations over time. These fluctuations are practically imprints of eddies flowing across the sampling volume. With point-measurements turbulence is quantified by the statistics of the fluctuations (e.g. variance), whereas the size of eddies is not measured.

On the other hand, whole-field measurement techniques, like Particle Image Velocimetry (PIV), provide velocity measurements on a large portion of the flow field simultaneously, so that they capture the spatial extent of flow structures (e.g. Adrian et al., 2000; Sokoray-Varga & Józsa, 2008). PIV measurements can be used to detect the motion of turbulent eddies, provided the temporal resolution of the measurement is high enough. Therefore the temporal and spatial resolutions of a PIV-system both determine the turbulent eddy scales that can be captured.

The present paper discusses the applicability of a PIV-system for detecting turbulent eddies in a vertical-slot fish pass. We give basic considerations on the parameters required by such measurement system and show the preliminary results from the scale model of a vertical-slot fish pass.

Experimental setup

In order to identify the characteristics of the flow and of the turbulent eddies in a vertical-slot fish pass, a physical model has been built in the laboratory of BAW.

The model comprises of 9 pools each 78 cm wide and 99 cm long. The width of the slot is 12 cm; the slope of the flume is 2.8 % (Fig. 1). The side walls and the bottom of the model are made of glass.
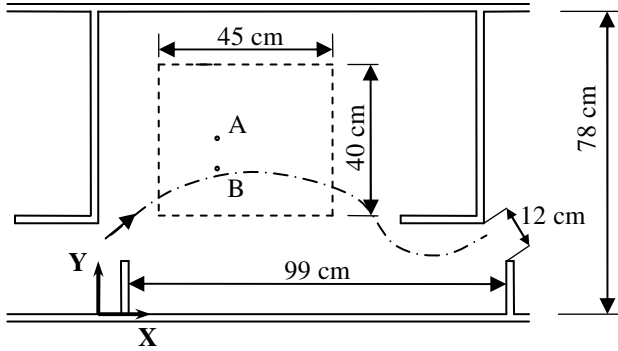

Figure 1: Plan view of a pool of the fish pass model. Dashed line: PIV measurement field; dashed-dot line: midline of the main stream; points A, B: ADV measurement points

The expected maximum velocity in the pools is expected downstream the slot with 0.75 m/s using equation (1), which is based on the head difference between the pools, Δh (e.g. Larinier, 1992; Wu et al., 1999; DWA, 2010). Therefore, the Reynolds number based on the maximum velocity and slot width in the model, is about $Re \sim 90\,000$.

$$v_{max} = \sqrt{2 \cdot g \cdot \Delta h} \tag{1}$$

The physical model is used to study the flow in several fish passes that are being planned along the Neckar River in Germany. The reduction scale for geometry is about 1:4. The dimensions followed the suggestions of the German design guideline (DWA, 2010).

It has to be noted that the design geometry of the present case study caused an unusual flow response in the pools. In contrast to the standard flow pattern expected in vertical-slot fish passes, consisting of a stable main stream and several recirculation cells, it was observed that the main stream interconnecting the slots oscillated. The midline of the main stream was practically migrating around the dashed-dot line shown in Figure 1.

The measurements presented in this paper were made in one pool of the fish pass model.

The Acoustic Doppler Velocimetry (ADV) measurements were taken at points A and B (Fig. 1) at 10 cm above the bottom by a down-looking Vectrino instrument (Nortek, 2000) with 200 Hz sampling rate and 10-minute measurement time duration.
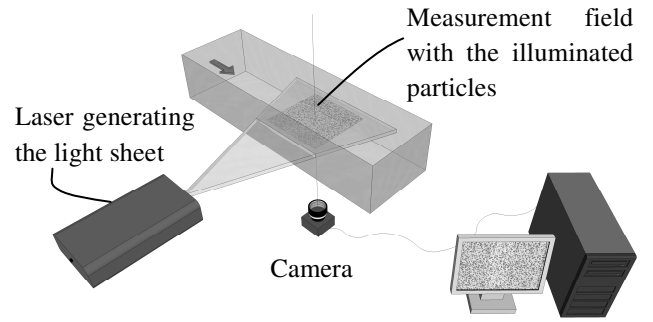

Figure 2: The schematic view of the PIV system

The two-dimensional Particle Image Velocimetry (PIV) measurements were carried out in the 45x40 cm large field sketched in Figure 1, at 10 cm above bottom by a PIV-system that was assembled in-house. The measurements were performed in a plane parallel to the bottom, containing the main velocity gradients of the flow, and thus the clearest evidence of the eddy development. The measurement field was illuminated through the side walls; the images were taken by a camera looking through the bottom of the model (Fig. 2).

The time-resolved PIV system worked a constant sampling rate of 200 Hz, and consisted mainly of a laser as light source, a camera with 1280x1024 pixels resolution at 200 frames per second, and a PC to record the images (Fig. 2).

The recordings were processed with a Particle Tracking Velocimetry (PTV) algorithm (Sokoray-Varga & Józsa, 2008). The scattered velocity field of each frame was interpolated to a predefined regular grid determining a regular velocity field for the frames. The variations of velocity at each grid point through the sequence of frames gave velocity time-series, to be processed in the same way as point measurements.

The eddy-detection method used in this study was the Swirling Strength Analysis, already adapted for two-dimensional velocity fields typical for PIV (Adrian et al., 2000). The detection is based on the eigenvalues of the velocity gradient tensor, whose imaginary part shows the strength of local swirling motion.

Considerations on the PIV system parameters

In brief, Particle Image Velocimetry (PIV) is an optical measurement technique, in which tracer particles are added to the flow and are illuminated by an intensive light. The illuminated flow region is then recorded by cameras. The local flow velocities are determined from the displacements of the illuminated particles between two subsequently recorded images (also called frames) and from the time delay between the frames. As a result, every pair of images delivers the instantaneous velocity vectors over the whole measurement field at one time.

One of the major challenges using PTV is the noise in the obtained velocities. Since the pixel resolution of the camera is limited, the individual particles are visible only on some pixels, in an optimal case on at least 3x3 pixels. Therefore, in order to attain usable vector fields the algorithms need to locate particle midpoints with sub-pixel accuracy. Such accuracy is achieved by estimator methods which introduce a little error in the location of the midpoints. This error results in small deviations in the particle displacements and in a high-frequency fluctuation in the velocity time-series. The resulting noise in PTV measurements is then filtered out by low-pass filters, which however produce "cleaned" times-series with an effective sampling rate lower than the nominal sampling frequency of the PIV-system. Consequently, the measurement system needs to have a higher nominal sampling rate than the frequencies of interest in the flow.

A PIV-system can only capture eddy sizes with the temporal and spatial resolutions achieved by the system specifications. Eddies of different sizes have different frequencies and the smaller the eddies, the higher their frequencies. On the one hand, the spatial resolution of the vector field determines the smallest eddy that can be captured spatially. On the other hand, the temporal resolution (sampling frequency) of the system should capture the frequencies associated with that eddy size. Consequently, both resolution parameters have to be adjusted simultaneously while capturing eddies.

Another challenge in detecting eddies is that eddies of different scales appear superimposed in the velocity fields and cannot be detected clearly. In order to determine the sizes of eddies the different scales need to be separated before eddy detection. The separation of the different scales is attained by applying frequency-based filters to the velocity time-series in all individual grid points. Since the frequency-based filtering does not involve neighboring grid points, the spatial extension of the eddies obtained with the filtered velocity fields is not affected by a spatial averaging. Therefore, in order to properly prepare the system for effective eddy detection, the expected scales of turbulence need to be estimated in advance. The energy spectra measured during the estimation are used for verifying the results of the PIV measurement.

The expected scales of turbulence in the pools

Here, the estimation of the turbulent scales is made based on turbulence theory for high Reynolds numbers (e.g. Pope, 2000; Davidson, 2004).

The turbulent flow field is composed of eddies of different sizes that occur superimposed in the flow field. Eddies can be characterized by their typical size (or length scale) l,

their typical velocity $u(l)$, and their typical time scale $\tau \sim l/u(l)$, which is their turn-over-time.

Characteristics of turbulent eddies of different sizes

Large scale turbulent eddies are created by mean flow instabilities. Their geometry is determined by the mean flow geometry and is affected by the geometry of the flow boundary. Their size (l_0) is comparable with the characteristic geometric length scales of the mean flow, and their geometry has directional biases; they are anisotropic.

Large eddies are unstable and break-up to smaller and smaller eddies. During this break-up process the geometrical characteristics (the directional biases) gradually vanish, so that eddies become statistically isotropic at a certain small size (l_{EI}), where the break-up process reaches a condition with universal characteristics, independent of the boundary geometry. Eddies in this range ($l < l_{EI}$) are in the so called universal equilibrium range (Fig. 3).

Therefore, the geometry of the large scale eddies is specific to the mean flow field and to the pool geometry, while these features are not present in the small scales. Once the large turbulent eddies (with $l > l_{EI}$) are captured in a fish pass, the scales in the universal range can be estimated well. Therefore, the large scales are object of the present measurements.
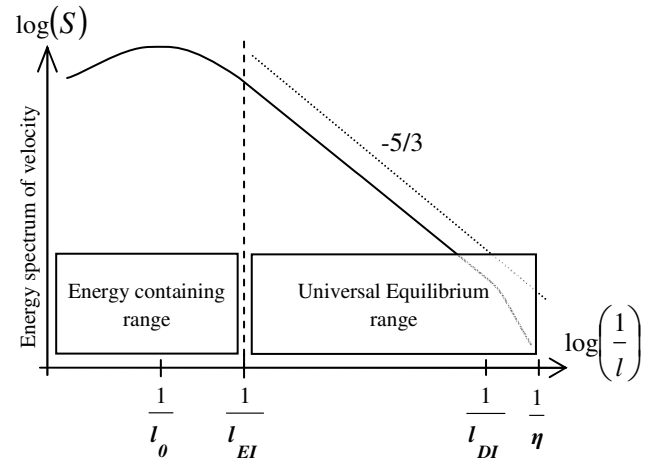

Figure 3: A typical energy spectrum function in fully developed turbulence, where l denotes the eddy size

The eddy break-up process also implies that kinetic energy is entered to turbulence by the mean flow at the largest eddies (production of turbulent energy), and is then transferred to smaller and smaller eddies. As the eddy sizes reach the universal range the distribution of the kinetic energy among the different eddy sizes reaches the universal function of power $-5/3$ known as the Kolmogorov $-5/3$ spectrum (Fig. 3). The universal range can be recognized on the $-5/3$ slope of the spectrum curve.

Note that this process is driven by inertial forces up to the size l_{DI} without significant loss of energy. Most of the

kinetic energy is only dissipated at eddy sizes below l_{DI}, near the Kolmogorov scale (η), where viscous forces can exert a significant action.

Estimation of the scales in the pools of the fish pass based on the standard deviation of the velocity

For the fish pass model, the characteristics of the large scale eddies were estimated based on the above theoretical approach and on the standard deviations of the flow velocity measured with the ADV.

In the fish pass, the characteristic length scale of the mean flow (l_0) is in the order of magnitude of 0.10 m (slot width: 0.12 m, water depth: 0.25 m). The characteristic velocity (u_0) of the large eddies has the order of magnitude of the standard deviation of the flow velocity. The ADV measurements performed at points A and B (Fig. 1) provided the standard deviation of 0.11 and 0.19 m/s respectively, which is in the order of magnitude of 0.10 m/s. With $u_0{\sim}0.10$ m/s, and $l_0{\sim}0.10$ m the order of magnitude of the typical time scale is $\tau_0{\sim}1$s, that is 1 Hz in frequency.

Since the length scale l_{EI} can be tentatively taken as being one order of magnitude smaller than l_0; this yields to about $l_{EI}{\sim}1$ cm. The eddy characteristics belonging to the length scale l_{EI} are then estimated using formulas (2) and (3). The typical velocity is $u_{EI}{\sim}0.05$ m/s and the typical time scale is $\tau_{EI}{\sim}0.2$ s, which is 5 Hz in frequency.

$$u(l) \sim u_0 \cdot (l/l_0)^{1/3} \tag{2}$$

$$\tau(l) \sim \tau_0 \cdot (l/l_0)^{2/3} \tag{3}$$

Measured energy spectrum in the fish pass model

The energy spectrum functions of the velocities have been generated (Fig. 4) using the velocity time-series measured by the ADV in points A and B (Fig. 1),

In case of the vertical velocity components (w), the $-5/3$ slope is reached around 2 Hz, which is indeed in the same order of magnitude as the estimated 5 Hz.

In case of the horizontal velocity components (u, v), the limit of the universal range is not as obvious. The spectrum of Figure 4 (a) shows clearly that the slope changes first to $-5/3$ at frequency of about 2 Hz, then it decreases and, it finally changes to $-5/3$ again around 20-30 Hz. A similar shape can be recognized in the velocity spectrum of point B (Fig. 4 (b)), although the slope after the second change cannot be determined, as frequencies above 100 Hz cannot be represented since the ADV sampling rate is 200 Hz.

The unusual variation of the slope of the energy spectrum functions suggests that there are multiple mean flow instabilities that feed the horizontal turbulence at two different "large scales", which appear superimposed in the measured energy spectrum functions.

Therefore, in order to capture all the geometry specific large scales in the pool, the PIV system should be able to deliver at least the frequency of l_{EI}. Based both on the estimations and on the measured energy spectra in point A, this frequency is approximately 20-30 Hz. In order to obtain this frequency in the measurements, the PIV-system should have an effective sampling rate of at least 40-60 Hz.
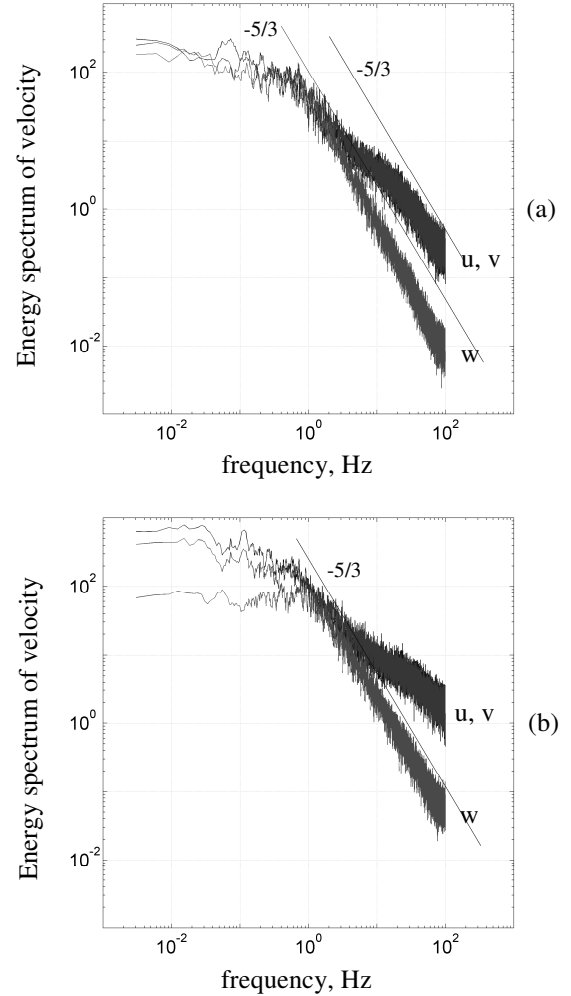

Figure 4: Measured energy spectra; (a) point A (b) point B

Results of a first PIV measurement

The first PIV measurement in the fish pass model delivered a 7 seconds long recording. The velocity fields used for present analyses were interpolated from the scattered velocity fields to a 1x1 cm regular grid.

The turbulence scale examined in this analysis is the largest scale detected in the energy spectra of the ADV measurements. The upper limit of this large scale range was around 2 Hz (Fig. 4), thus the velocity time-series were low-pass filtered with a frequency cutoff of 2.5 Hz.

The oscillations of the main stream can be clearly recognized in the low-pass filtered recordings. The main stream migrates in y-direction in an approximately periodic way. In order to visualize this, the outermost positions of

the main stream have been displayed using the velocity fields of Figure 5: Figure 5(a) the main stream midline at y=0.35 m, Figure (b) at y=0.30 m and Figure 5(c) at y=0.35 m again. This oscillation has a time period of about 1.7 seconds (0.6 Hz).
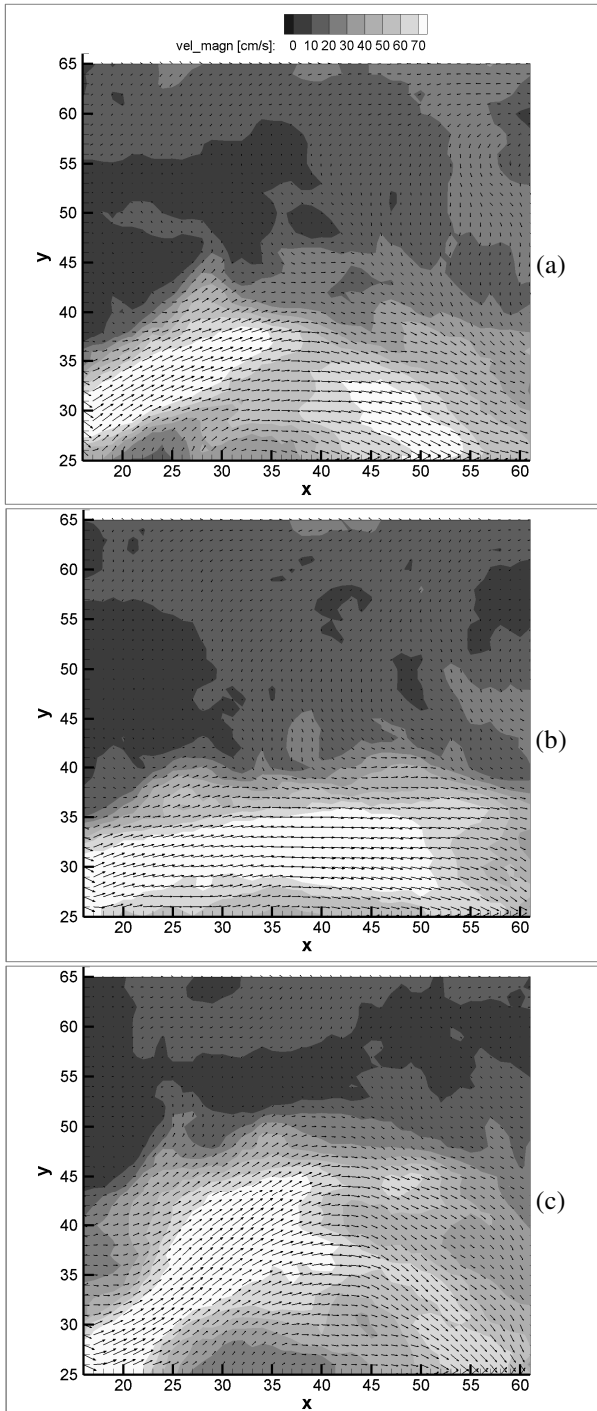

Figure 5: Instantaneous velocity fields after low pass filtering: (a) at 4.65 s, (b) at 5.50 s and (c) at 6.35 seconds. The coordinate system is shown in Figure 1.

These velocity fields were then used for the eddy detection based on the swirling strength concept mentioned earlier. Large scale eddies can be visualized clearly in all frames

and their evolution can be followed closely (Figure 6). It can be observed that some of them maintain their identity over a longer lifetime (eddy "A" in Figure 6), while others disappear quite quickly (eddy "B" in Figure 6).
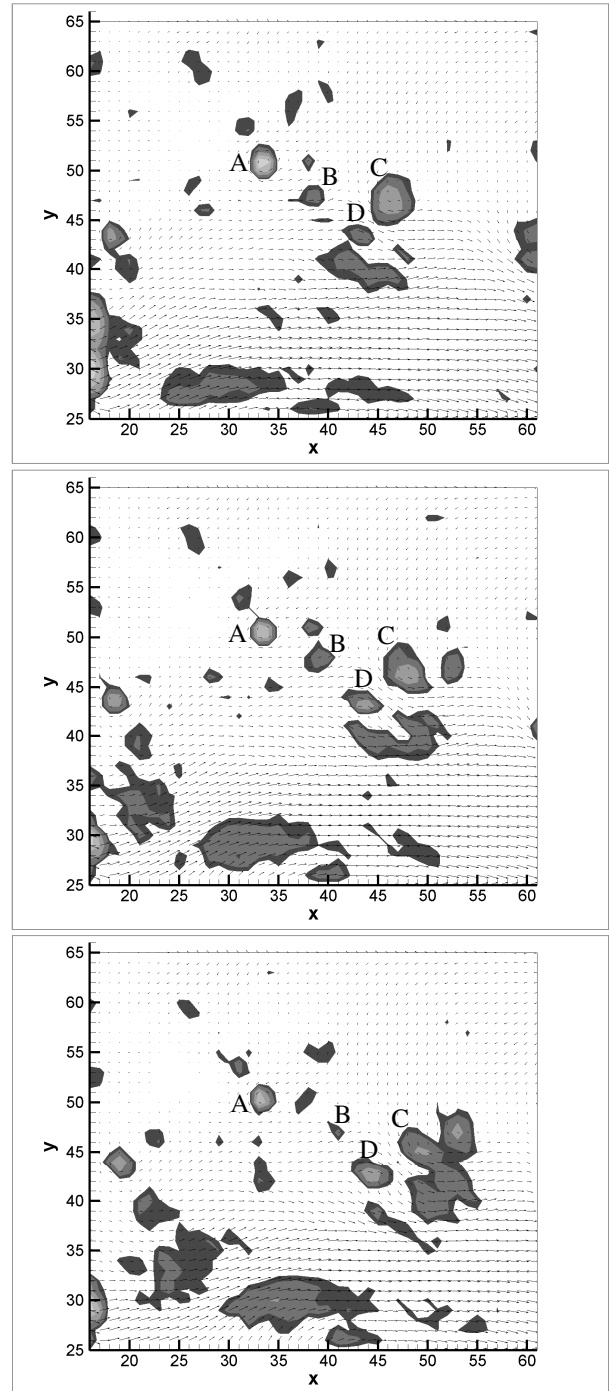

Figure 6: Eddy detection in a series of frames. Time separation between frames is 0.1 seconds.

Discussion

We argue that the oscillating main stream shown in Figure 5 is one reason for the multiple flow instabilities appearing in the measured energy spectra of Figure 4, since the oscillation has a frequency of about 0.6 Hz and the energy

spectra show their first "peaks" near this frequency. The reason for the second "peaks" could be the instability due to the shear between the main stream and the slower flow beside. For a conclusive analysis, however, longer measurements and velocity fields interpolated to finer grids are needed.

The presented results are based on velocity fields interpolated on a regular grid with 1x1 cm spacing and with a frequency cutoff of 2.5 Hz. This is sufficient to detect large eddies, but the grid spacing should be finer in order to enhance the accuracy in the determination of the eddy size. In order to detect eddies of smaller scales, both the spacing of the interpolation grid and the filtering frequency should be adjusted to the examined eddy scales. Additionally, when using a PTV algorithm, the grid spacing has also to be adjusted to the density of the velocity vectors in the frames.

It must be noted that the flow in a vertical-slot fish pass is three-dimensional. The velocity fields provided by just one camera are not the accurate two-dimensional velocities, as they may also include an out-of-plane velocity component due to the perspective projection. For more accurate measurements the out-of-plane velocity component should be estimated by using a second camera.

Conclusions

The presented results demonstrated that the used PIV-system and the methodology for the data evaluation can be successfully applied for capturing turbulent eddies in a fish pass model.

The measured energy spectra have shown that in order to capture the velocity fluctuations of all the geometry specific large scale eddies in the scale model the measurement system should have an effective sampling rate of at least 60 Hz, but some regions might require even higher sampling rates.

As eddies of different sizes appear superimposed in the velocity fields and cannot be detected clearly, a distinct range of scales was separated, and was examined separately by the swirling strength eddy detection algorithm. The separation of the scales was achieved by applying frequency based filters on the velocity time-series in each individual grid point of the velocity fields.

The present methodology will also make it possible to examine different geometrical variants of the fish pass, in order to reveal the characteristics of the turbulent eddies within the pools. Moreover, determining the scales and characteristics of turbulent eddies in a quantitative way will contribute to a better interpretation of fish behavior, and to the improvement of the design guidelines for fish passes.

References

Adrian, R.J., Christensen, K.T. & Liu, Z.-C. (2000). Analysis and interpretation of instantaneous turbulent velocity fields, *Experiments in Fluids*, Vol. 29, pp. 275-290

Bleckmann, H., Mogdans, J., Engelmann, J., Kröther, S. & Hanke, W. (2004). Das Seitenliniensystem - Wie Fische Wasser fühlen, *Biologie in. Unserer Zeit*, Vol. 6, pp. 358-365

Davidson, P.A. (2004). *Turbulence, an introduction for scientists and engineers*, Oxford University Press

DWA (2010) *Fischaufstiegsanlagen und fischpassierbare Bauwerke - Gestaltung, Bemessung, Qualitätssicherung – Entwurf*, DWA-M 509, DWA

Enders, E.C., Boisclair, D. & Roy, A.G. (2003). The effect of turbulence on the cost of swimming for juvenile Atlantic salmon (Salmo salar), *Canadian Journal of Fisheries and Aquatic Sciences*, Vol. 60, pp. 1149-1160

Larinier, M. (1992). Passes a bassins successifs, prebarrages et rivieres artificielles, *Bulletin Francais de Peche et Pisciculture*, Vol. 326-327, pp. 45-72

Liao, J.C., Beal, D.N., Lauder, G.V. & Triantafyllou, M.S. (2003). Fish Exploiting Vortices Decrease Muscle Activity, *Science*, Vol. 302(5650), pp. 1566-1569

Liao, J.C. (2007). A review of fish swimming mechanics and behaviour in altered flows, *Philosophical Transactions of the Royal Society B*, Vol. 362, pp. 1973–1993

Liu, M., Rajaratnam, N. & Zhu, D.Z. (2006). Mean flow and turbulence structure in vertical slot fishways, *Journal Of Hydraulic Engineering*, Vol. 132, pp. 765-777

Nikora, V., Aberle, J., Jowett, I., Biggs, B. & Sykes, J. (2003). On turbulence effects on fish swimming performance: a case study of the new zealand native fish galaxias maculatus (inanga), *XXX IAHR Congress Proceedings*, pp. 425-432

Nortek (2009), *Vectrino Velocimeter Manual*, Nortek AS

Pope, S.B. (2000). *Trubulent Flows*, Cambridge University Press

Przybilla, A., Kunze, S., Rudert, A., Bleckmann, H. & Brucker, C. (2010). Entraining in trout: a behavioural and hydrodynamic analysis, *Journal Of Experimental Biology*, Vol. 213, pp. 2976-2986

Puertas, J., Pena, L. & Teijeiro, T. (2004). Experimental Approach to the Hydraulics of Vertical Slot Fishways, *Journal Of Hydraulic Engineering*, Vol. 130, pp. 10-23

Silva, A.T., Santos, J.M., Ferreira, M.T., Pinheiro, A.N. & Katopodis, C. (2011). Effects of water velocity and turbulence on the behaviour of Iberian barbel (Luciobarbus bocagei, Steindachner 1864) in an experimental pool-type fishway, *River Research and Applications*, John Wiley & Sons, Ltd., Vol. 27(3), pp. 360-373

Smith, D.L., Brannon, E.L. & Odeh, M. (2005). Response of Juvenile Rainbow Trout to Turbulence Produced by Prismatoidal Shapes, *Transactions of the American Fisheries Society*, Vol. 134(3), pp. 741 - 753

Sokoray-Varga, B. & Jozsa, J. (2008). Particle tracking velocimetry (PTV) and its application to analyse free surface flows in laboratory scale models, *Periodica Polytechnica Civil Engineering*, Vol. 52/2, pp. 63–71

Tarrade, L., Texier, A., David, L. & Larinier, M. (2008). Topologies and measurements of turbulent flow in vertical slot fishways, *Hydrobiologia*, Vol. 609, pp. 177–188

Tritico, H.M. & Cotel, A.J. (2010). The effects of turbulent eddies on the stability and critical swimming speed of creek chub (Semotilus atromaculatus), *Journal Of Experimental Biology*, Vol. 213(13), pp. 2284-2293

Webb, P. (1998). Entrainment by river chub Nocomis micropogon and smallmouth bass Micropterus dolomieu on cylinders, *Journal Of Experimental Biology*, Company Of Biologists Ltd, Vol. 201(16), pp. 2403-2412

Wu, S., Rajaratnam, N. & Katopodis, C. (1999). Structure of flow in a vertical slot fishway, *Journal of Hydraulic Engineering*, Vol. 125(4), pp. 351-359